Article

pubs.acs.org/Biomac

Light-Triggered Concomitant Enhancement of Magnetic Resonance Imaging Contrast Performance and Drug Release Rate of Functionalized Amphiphilic Diblock Copolymer Micelles

Yamin Li,[†] Yinfeng Qian,[‡] Tao Liu,[†] Guoying Zhang,[†] and Shiyong Liu*,[†]

[†]CAS Key Laboratory of Soft Matter Chemistry, Hefei National Laboratory for Physical Sciences at the Microscale, Department of Polymer Science and Engineering, University of Science and Technology of China, Hefei, Anhui 230026, China

[‡]The First Affiliated Hospital of Anhui Medical University, Hefei, Anhui 230022, China

Supporting Information

ABSTRACT: Polymeric drug nanocarriers integrated with diagnostic and sensing functions are capable of in situ monitoring the biodistribution of chemotherapeutic drugs and imaging/contrasting agents, which enables the establishment of image-guided personalized cancer therapeutic protocols. Responsive multifunctional theranostic nanocarriers possessing external stimuli-tunable drug release rates and imaging signal intensities represent another promising direction in this field. In this work, we fabricated responsive amphiphilic diblock copolymer micelles exhibiting light-triggered hydrophobic−hydrophilic transition within micellar cores and the concomitant enhancement of magnetic resonance (MR) imaging contrast performance and release rate of physically encapsulated hydrophobic drugs. POEGMA-*b*-P(NIPAM-*co*-NBA-*co*-*Gd*) diblock copolymer covalently labeled with Gd^{3+} complex (*Gd*) in the light-responsive block was synthesized at first, where OEGMA, NIPAM, and NBA are oligo(ethylene glycol) monomethyl ether methacrylate, *N*-isopropylacrylamide, and *o*-nitrobenzyl acrylate, respectively. The amphiphilic diblock copolymer spontaneously self-assembles in aqueous solution into micellar nanoparticles possessing hydrophobic P(NIPAM-*co*-NBA-*co*-*Gd*) cores and hydrophilic POEGMA coronas, which can physically encapsulate doxorubicin (Dox) as a model chemotherapeutic drug. Upon UV irradiation, hydrophobic NBA moieties within micellar cores transform into hydrophilic carboxyl derivatives, triggering micelle microstructural changes and core swelling. During this process, the microenvironment surrounding Gd^{3+} complexes was subjected to a transition from being hydrophobic to hydrophilic, leading to the enhancement of MR imaging contrast performance, that is, ∼1.9-fold increase in longitudinal relaxivity (r_1). In addition, the release rate of encapsulated Dox was also enhanced (∼65% of Dox release in 12 h upon UV irradiation versus ∼47% Dox release in 25 h for the control). The reported strategy of light-triggered coenhancement of MR imaging contrast performance and drug release profiles represents a general route to the construction of next generation smart polymeric theranostic nanocarriers.

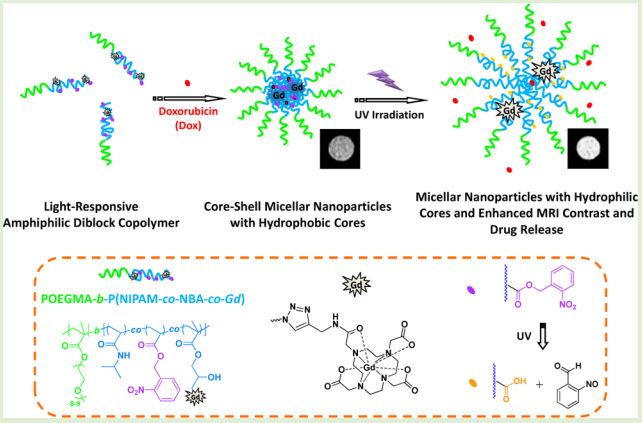

INTRODUCTION

In the past decades, magnetic resonance (MR) imaging has emerged to be a competitive and powerful diagnostic tool due to its noninvasiveness, capability of differentiating soft tissues of varying physiological conditions, and high lateral and depth resolution.[1−4] To improve the diagnostic accuracy, a variety of MR imaging contrast agents have been developed including well-established paramagnetic Gd^{3+}-based T_1 agents and super-para-magnetic iron oxide (SPIO) nanoparticle-based T_2 agents, which can increase the longitudinal and transverse relaxation rate of surrounding water protons, respectively.[5−7] Therefore, positive or negative MR imaging contrast enhancement can be achieved in the presence of contrast agents.

In recent years, increasing attention has been paid to small molecule-based responsive MR imaging contrast agents.[8−12] Changes in MR signal intensity can be actuated upon exerting a specific stimulus of interest such as pH, metal ions, proteins, and enzymes. In principle, the external stimuli-modulation of MR signal intensity can be achieved by utilizing three main strategies according to the theory of Solomon−Bloembergen−Morgan (SBM), namely, modifying the number of water molecules bound to paramagnetic ions (q), tuning the lifetime of bound water (τ_m), and changing the rotational correlation time (τ_r).[3] In this context, Meade and coworkers pioneered a new type of smart MR imaging contrast agent based on Gd^{3+} complex for the detection of β-galactosidase activity.[13] Lippard

Received: September 12, 2012
Revised: September 26, 2012
Published: September 27, 2012

Scheme 1. Schematic Illustration for the Fabrication of Light-Responsive Polymeric Micelles of POEGMA-*b*-P(NIPAM-*co*-NBA-*co*-*Gd*) Amphiphilic Diblock Copolymer Exhibiting Light-Triggered Hydrophobic−hydrophilic Transition within Micellar Cores and the Concomitant Enhancement of Magnetic Resonance (MR) Imaging Contrast Performance and Release Rate of Physically Encapsulated Hydrophobic Drugs (Dox)

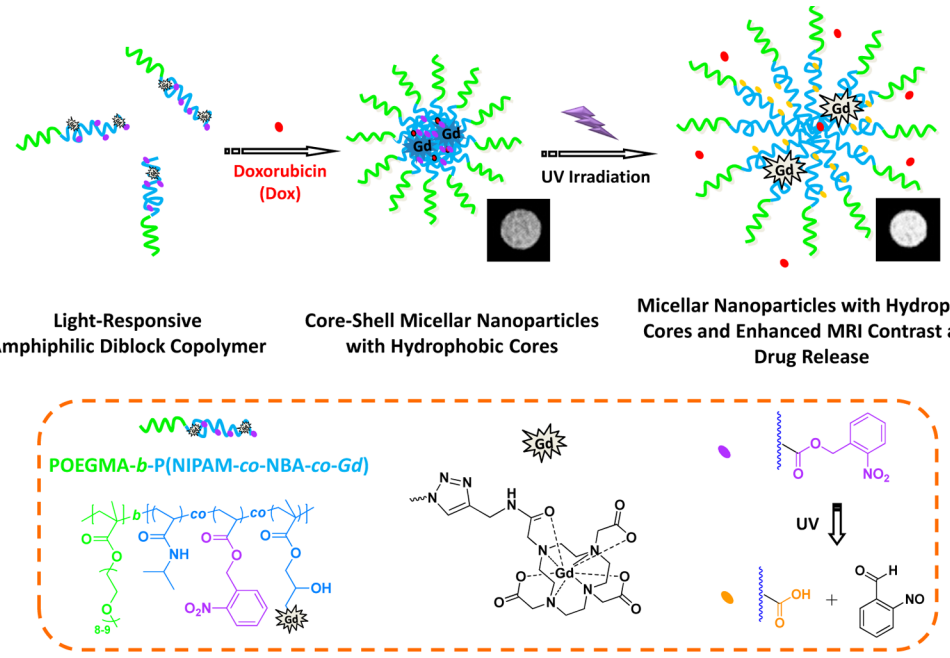

Scheme 2. Synthetic Routes Employed for the Preparation of POEGMA-*b*-P(NIPAM-*co*- NBA-*co*-*Gd*) Diblock Copolymer via the Combination of Consecutive RAFT Polymerizations and "Click" Post-Functionalization

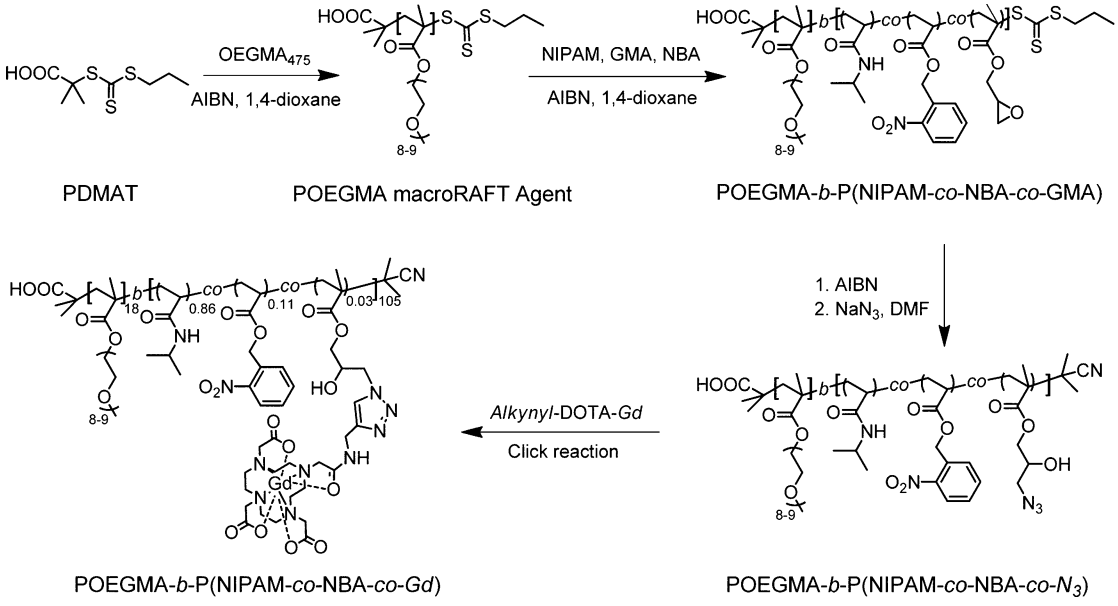

et al.[14] developed an elegant Zn^{2+}-responsive MR imaging contrast agent based on Mn^{2+} complex. In addition to external stimuli-tunable T_1 contrast agents, responsive T_2 ones could also be constructed, as reported by Jasanoff et al.[15] on the basis of protein-coated SPIO nanoparticles; in their work, Ca^{2+}-mediated protein−protein interactions can lead to nanoparticle clustering and concomitant increase of T_2 relaxivity. Other modulation techniques such as light irradiation in the UV, visible, or NIR range can also be utilized.[16−23] For example, Louie and coworkers developed a series of small molecule photoresponsive T_1 and T_2 contrast agents bearing spiropyran derivatives as the antenna, and thus both relaxation rates can be facilely tuned by light irradiation.[24,25]

It is worth noting that the above examples of responsive MR imaging contrast agents are exclusively based on small molecules or SPIO nanoparticles. Polymeric nanoparticles and block copolymer assemblies have recently emerged to be an excellent candidate for constructing nanocarriers of therapeutic drugs and imaging agents.[26−28] Compared with small molecule drugs, drug conjugates, and imaging/contrast agents, polymeric assemblies and nanoparticles exhibit extended blood circulation duration and improved accumu-

dx.doi.org/10.1021/bm301425j | *Biomacromolecules* 2012, 13, 3877−3886

lation within disease sites such as tumor tissues due to the enhanced permeation and retention (EPR) effect.[29] In particular, if polymeric nanoparticles or assemblies are physically loaded or covalently anchored with drugs and imaging/contrast agents, then they can possess combined functions of chemotherapy and diagnostics/sensing. The above integration has led to the new concept of "theranostics" or "image-guided therapy".[30−35]

Responsive MR imaging contrast agents based on block copolymer assemblies such as micelles have been rarely explored.[36,37] Inspired by the work of Meade[13] and Hamachi[38] research groups concerning enzyme-responsive modulation of MR signal intensity of small molecule contrast agents and based on our past experience in stimuli-responsive polymers and polymeric assemblies,[39,40] we hypothesized that if Gd^{3+} complex, serving as T_1-type contrast agent, is covalently attached onto the hydrophobic block of amphiphilic block copolymers, then Gd^{3+} complex will be initially located within hydrophobic cores of self-assembled micelles, which might effectively suppress T_1 relaxation rate. If the hydrophobic block within micellar cores is subjected to light irradiation or enzyme-triggered chemical reactions and rendered to be hydrophilic, then the incurred microstructural changes of polymeric micelles will lead to the transition of microenvironments surrounding Gd^{3+} complex from being hydrophobic to hydrophilic. This might lead to the prominent increase in MR signal intensities due to enhanced exchange between Gd^{3+} complex and water molecules. Moreover, if hydrophobic drugs are initially encapsulated within polymeric micelles, then the above external stimuli-induced hydrophobic−hydrophilic transition within micellar cores will also lead to triggered drug release.

On the basis of the above assumption, we attempted to fabricate UV irradiation-responsive polymeric micelles of POEGMA-*b*-P(NIPAM-*co*-NBA-*co*-*Gd*) amphiphilic diblock copolymer, where OEGMA, NIPAM, and NBA represent oligo(ethylene glycol) monomethyl ether methacrylate, *N*-isopropylacrylamide, and *o*-nitrobenzyl acrylate, respectively (Schemes 1 and 2). A model chemotherapeutic drug, doxorubicin (Dox), was loaded into the hydrophobic P(NIPAM-*co*-NBA-*co*-*Gd*) core of micellar nanoparticles. Upon UV irradiation, the photocleavage of NBA moieties leads to a hydrophobic−hydrophilic transition for micellar cores. The effects of phototriggered microstructural transition on the drug release rate and T_1-type MR imaging contrast performance were then investigated. It turns out that light-triggered concomitant enhancement of MR imaging contrast performance and drug release rate can be achieved.

MATERIALS AND METHODS

Materials. Oligo(ethylene glycol) monomethyl ether methacrylate ($OEGMA_{475}$, M_n = 475 g/mol, mean degree of polymerization, DP, is 8 to 9) purchased from Aldrich was passed through a neutral alumina column to remove the inhibitor and then stored at −20 °C prior to use. *N*-Isopropylacrylamide (NIPAM, 97%, Tokyo Kasei Kagyo) was recrystallized twice from a mixture of benzene and *n*-hexane (1/3, v/v) and then stored at −20 °C prior to use. Glycidyl methacrylate (GMA, 98%, Aldrich) was dried over calcium hydride (CaH_2), vacuum-distilled, purged with nitrogen, and stored at −20 °C prior to use. 2,2′-Azoisobutyronitrile (AIBN) was recrystallized from 95% ethanol. Doxorubicin hydrochloride (Dox·HCl) was purchased from Aldrich and used as received. *N*,*N*,*N*′,*N*″,*N*″-Pentamethyldiethylenetriamine (PMDETA, 98%, Aldrich), copper(I) bromide (CuBr, 98%, Aldrich), ammonium chloride (NH_4Cl, Sinopharm Chemical Reagent), *o*-nitrobenzyl alcohol, sodium azide (NaN_3, 99%, Alfa Aesar), and all other reagents were used as received. Fetal bovine serum (FBS), penicillin, streptomycin, and Dulbecco's modified Eagle's medium (DMEM) were purchased from GIBCO and used as received. Triethylamine (TEA) and dichloromethane (DCM) were dried over CaH_2 and distilled prior to use. Acryloyl chloride (Sinopharm Chemical Reagent) was distilled under reduced pressure prior to use. Water was deionized with a Milli-Q SP reagent water system (Millipore) to a specific resistivity of 18.4 MΩ·cm. Alkynyl-functionalized DOTA-*Gd* complex, *alkynyl*-DOTA-*Gd* (DOTA is 1,4,7,10-tetraaza-cyclododecane-1,4,7,10- tetrakisacetic acid). and *S*-1-propyl-*S*′-(*α*,*α*′-dimethyl-*α*″-acetic acid)trithiocarbonate (PDMAT) were synthesized according to previous literature procedures.[41,42]

Sample Preparation. Synthetic routes employed for the preparation of light-responsive amphiphilic diblock copolymers, POEGMA-*b*-P(NIPAM-*co*-NBA-*co*-*Gd*), are shown in Scheme 2.

Synthesis of POEGMA macroRAFT Agent (Scheme 2). $OEGMA_{475}$ (2.0 g, 4.2 mmol), PDMAT (50 mg, 0.2 mmol), AIBN (6.9 mg, 0.04 mmol), and 1,4-dioxane (2 mL) were charged into a reaction tube equipped with a magnetic stirring bar. The tube was carefully degassed by three freeze−pump−thaw cycles and then sealed under vacuum. After thermostatting at 70 °C in an oil bath and stirring for 7 h, the reaction tube was quenched into liquid nitrogen, opened, and diluted with THF; the mixture was then precipitated into an excess of cold diethyl ether. The above dissolution−precipitation cycle was repeated three times. After drying in a vacuum oven overnight at room temperature, POEGMA was obtained as yellow viscous liquid (0.96 g, yield: 48%). The molecular weight and molecular weight distribution of POEGMA were determined by GPC using THF as the eluent, revealing an M_n of 5.6 kDa and an M_w/M_n of 1.30 (Figure 1a).

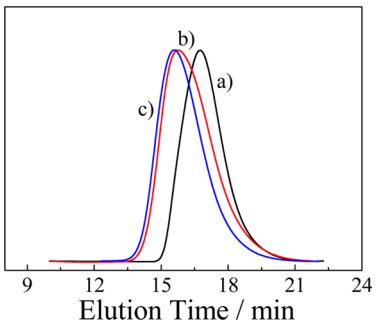

Figure 1. THF GPC traces recorded for (a) POEGMA macroRAFT agent ($M_{n,GPC}$ = 5.6 kDa, M_w/M_n = 1.30), (b) POEGMA-*b*-P(NIPAM-*co*-NBA-*co*-GMA) ($M_{n,GPC}$ = 10.6 kDa, M_w/M_n = 1.40), and (c) POEGMA-*b*-P(NIPAM-*co*-NBA-*co*-*Gd*) ($M_{n,GPC}$ = 13.4 kDa, M_w/M_n = 1.34).

Because of that the terminal trithiocarbonate moiety lacks characteristic ^1H NMR resonance peaks, the actual DP of POEGMA was estimated to be ∼18 based on the monomer conversion of $OEGMA_{475}$ (86%), as determined by ^1H NMR analysis for the crude polymerization mixture before purification. Therefore, the macroRAFT agent was denoted as $POEGMA_{18}$.

Synthesis of POEGMA-*b*-P(NIPAM-*co*-NBA-*co*-GMA) Block Copolymers (Scheme 2). The photoresponsive monomer, NBA, was synthesized according to literature procedures and characterized by ^1H NMR analysis in $CDCl_3$ (Figure S1a of the Supporting Information).[43−45] $POEGMA_{18}$ (0.29 g, 0.03 mmol), NIPAM (1.0 g, 8.8 mmol), NBA (0.14 g, 0.68 mmol), GMA (0.02 g, 0.14 mmol), AIBN (1.3 mg, 0.008 mmol), and 1,4-dioxane (1.5 mL) were charged into a glass ampule equipped with a magnetic stirring bar. The tube was carefully degassed by three freeze−pump−thaw cycles and then sealed under vacuum. After thermostatting at 70 °C in an oil bath and stirring for 24 h, the reaction tube was quenched into liquid nitrogen, opened, and diluted with THF; the mixture was then precipitated into an excess of diethyl ether. The above dissolution−precipitation cycle was repeated for three times. After drying in a vacuum oven overnight at room temperature, POEGMA-*b*-P(NIPAM-*co*-NBA-*co*-GMA) was

dx.doi.org/10.1021/bm301425j | *Biomacromolecules* 2012, 13, 3877−3886

obtained as light yellowish powder (0.33 g, yield: 23%). GPC analysis revealed an M_n of 10.6 kDa and an M_w/M_n of 1.40 (Figure 1b). DP of the photoresponsive block was determined to be 105 and molar fractions of NIPAM, NBA, and GMA moieties were determined to 0.86, 0.11, and 0.03 by ^{1}H NMR analysis in $CDCl_3$ (Figure S1b of the Supporting Information). The polymer was denoted as POEGMA$_{18}$-*b*-P(NIPAM$_{0.86}$-*co*-NBA$_{0.11}$-*co*-GMA$_{0.03}$)$_{105}$.

Synthesis of POEGMA-*b*-P(NIPAM-*co*-NBA-*co*-Gd) Amphiphilic Diblock Copolymers (Scheme 2). The ring-opening reaction of pendent epoxide functionalities in GMA units of POEGMA-*b*-P(NIPAM-*co*-NBA-*co*-GMA) diblock copolymer with NaN_3 was conducted as follows.[46] At first, POEGMA-*b*-P(NIPAM-*co*-NBA-*co*-GMA) diblock copolymer was treated with an excess of AIBN (10.0 equiv) in 1,4-dioxane to remove terminal trithiocarbonate moieties. After stirring at 70 °C for 2 h, the diblock copolymer was precipitated into an excess of diethyl ether for three times and dried overnight in a vacuum oven at room temperature. Subsequently, the diblock copolymer (7.5 g, 1.1 mmol epoxide moieties), NaN_3 (0.21 g, 3.2 mmol), and ammonium chloride (0.17 g, 3.2 mmol) were added to 20 mL DMF. The mixture was stirred at 50 °C for 24 h. After removing insoluble salts by filtration, the filtrates were directly dialyzed (cellulose membrane, molecular weight cutoff, 3.5 kDa) against deionized water for 12 h; fresh water was replaced every ∼4 h. The product was obtained by lyophilization (6.8 g, yield: 90%) and denoted as POEGMA-*b*-P(NIPAM-*co*-NBA-*co*-N_3). THF GPC characterization revealed an M_n of 10.8 kDa and an M_w/M_n of 1.40.

In the next step, POEGMA-*b*-P(NIPAM-*co*-NBA-*co*-*Gd*) was synthesized via the "click" postfunctionalization of POEGMA-*b*-P(NIPAM-*co*-NBA-*co*-N_3) precursor with *alkynyl*-DOTA-*Gd*. In a typical procedure, POEGMA-*b*-P(NIPAM-*co*-NBA-*co*-N_3) (0.69 g, 0.10 mmol azide moieties), *alkynyl*-DOTA-*Gd* (0.18 g, 0.30 mmol), PMDETA (17 mg, 0.10 mmol), and DMF (3.2 mL) were charged into a glass ampule equipped with a magnetic stirring bar. The mixture was degassed by three freeze−pump−thaw cycles; then, CuBr (14 mg, 0.10 mmol) was introduced under nitrogen atmosphere. After thermostatting at 50 °C in an oil bath and stirring for 24 h, the reaction tube was quenched into liquid N_2, opened, and exposed to air, and diluted with THF. The reaction mixture was then passed through an alumina column using THF as the eluent to remove copper catalysts. After removing all solvents on a rotary evaporator, the residues were dissolved in THF and then dialyzed (molecular weight cutoff, 3.5 kDa) against deionized water for 12 h; fresh water was replaced every ∼4 h. The final product was obtained by lyophilization (0.67 g, yield: 89%). GPC characterization revealed an M_n of 13.4 kDa and an M_w/M_n of 1.34 (Figure 1c). The Gd^{3+} content within the block copolymer was determined to be 2.1 wt % by inductively coupled plasma atomic emission spectrometry (ICP-AES) measurement, corresponding to ∼3 DOTA-*Gd* complex per chain. Therefore, the polymer was denoted as POEGMA$_{18}$-*b*-P(NIPAM$_{0.86}$-*co*-NBA$_{0.11}$-*co*-*Gd*$_{0.03}$)$_{105}$ and shortened as POEGMA-*b*-P(NIPAM-*co*-NBA-*co*-*Gd*) in subsequent sections.

Preparation of Micellar Solution. In a typical procedure,[40] 10 mg of POEGMA-*b*-P(NIPAM-*co*-NBA-*co*-*Gd*) diblock copolymer was dissolved in 1 mL of DMSO. Under vigorous stirring, 9 mL of deionized water was introduced at a rate of 0.1 mL/min. After the addition process is completed, the mixture was further stirred for 2 h. DMSO was then removed by dialysis (cellulose membrane, molecular weight cutoff, 7.0 kDa) against deionized water for 12 h, and fresh water was replaced every ∼4 h. Stock solution with a bluish tinge characteristic of colloidal dispersion was obtained, suggesting the formation of polymeric micelles.

Determination of Critical Micellization Concentration (CMC). The fluorescence probe method was used to determine the CMC of POEGMA-*b*-P(NIPAM-*co*-NBA-*co*-*Gd*) micelles.[47] A predetermined amount of pyrene solution in acetone was added to a series of volumetric flasks, and acetone was then evaporated completely under vacuum. A series of copolymer solutions at varying concentrations were added to the flasks, and the final pyrene concentration in each flask was fixed at 6.0×10^{-7} mol L^{-1}. The excitation spectra were recorded at 25 °C on a spectrofluorometer with λ_{em} at 390 nm and a slit width of 5 nm.

Preparation of Nile Red-Loaded Micelles and Light-Triggered Release of Nile Red. In a typical procedure,[48] 10 μL of Nile red stock solution in acetone was added to an empty vial, which was then placed in a vacuum oven to remove the solvent. A calculated amount of stock micellar solution (1.0 g/L) was added to the vial, and the final concentration of Nile red was adjusted to 6.6×10^{-7} mol L^{-1}. Upon UV irradiation (365 nm, 1.0 mW/cm^2) for varying time durations, the emission spectra of Nile red-loaded micellar solution were then recorded.

Preparation of Dox-Loaded Micelles. A mixture of Dox·HCl (2.5 mg), TEA (0.5 mL), and DMSO (2.5 mL) was stirred for 2 h and 10.0 mg POEGMA$_{18}$-*b*-P(NIPAM$_{0.86}$-*co*- NBA$_{0.11}$-*co*-*Gd*$_{0.03}$)$_{105}$ diblock copolymer was then added. The solution was subjected to dialysis against PBS buffer (pH 7.4) at room temperature for 12 h, and the external buffer solution was refreshed every 4 h during this period. After completing this process, the polymer concentration was adjusted to 1.0 g/L for the subsequent in vitro drug release experiments. The amount of unloaded Dox in the dialysates was determined by fluorescence method against a standard calibration curve. The encapsulation efficiency (EE%) and the loading content (LC%) were calculated according to previous literature reports.[40]

In Vitro Dox Release. 100 μL of aqueous dispersion of drug-loaded micelles (1.0 g/L) was transferred to a dialysis cell with a molecular weight cutoff of 2.0 kDa and then dialyzed against 3.4 mL of PBS buffer (pH 7.4) at 37 °C. The sample was irradiated by UV light for 30 min. The control sample was dialyzed in the dark. The Dox concentration in the dialysate was quantified by measuring the fluorescence emission of doxorubicin at 595 nm (λ_{ex} = 495 nm) against a standard calibration curve.[49−52]

In Vitro Cytotoxicity Measurement. Cell viability was examined by the MTT assay. HepG2 cells were seeded in a 96-well plate at an initial density of 5000 cells/well in 100 μL of complete DMEM medium. Drug-loaded micelles with and without 30 min UV irradiation were then added to target a final concentration of 3.0 mg/mL. After incubating for 24 h, MTT reagent (in 20 μL PBS buffer, 5 mg/mL) was added to each well, and the cells were further incubated with 5% CO_2 for 4 h at 37 °C. The culture medium in each well was removed and replaced by 150 μL of DMSO. The solution from each well was transferred to another 96-well plate, and the absorbance values were recorded at a wavelength of 490 nm by a microplate reader (Thermo Fisher). The cell viability is calculated to be $A_{490,treated}/A_{490,control} \times 100\%$, where $A_{490,treated}$ and $A_{490,control}$ are the absorbance values in the presence and absence of polymeric micelles, respectively. Each experiment was done in quadruple, and the data are shown as the mean value plus a standard deviation (±SD).

In Vitro MRI Relaxivity Measurement. The longitudinal relaxation rates ($1/T_1$) of POEGMA-*b*-P(NIPAM-*co*-NBA-*co*-*Gd*) micelles and small molecule contrast agent, *alkynyl*-DOTA-*Gd*, in PBS buffer (pH 7.4) at varying Gd^{3+} concentrations (0, 0.01, 0.02, 0.03, and 0.04 mM) before and after UV irradiation were acquired at room temperature using GE Signa Horizon 1.5 T MR scanner equipped with a human head coil. Conventional spin−echo pulse sequence was used for T_1 measurements with a single slice thickness of 4 mm, field of view (FOV) of 10 × 10 cm, and matrix size of 128 × 128. The repetition times (TRs) were 300, 400, 500, 600, 800, 1000, 1500, and 2000 ms with an echo time (TE) of 10 ms. The net magnetizations for each sample were determined from the selected region of interest (ROI) and fitted to the following multiparametric nonlinear regression function: $M_{TR} = M_0\,(1 - e^{-TR/T1})$, where M_{TR} denotes the measured signal intensity as a function of TR and M_0 is the signal intensity in the thermal equilibrium. T_1 was calculated from these data using a MATLAB program, and longitudinal relaxivity r_1 was determined from the slope of $1/T_1$ versus $[Gd^{3+}]$ plot.

Characterization. All nuclear magnetic resonance (NMR) spectra were recorded on a Bruker AV300 NMR 300 MHz spectrometer operated in the Fourier transform mode. $CDCl_3$ was used as the solvent. Molecular weights and molecular weight distributions were determined by gel permeation chromatography (GPC) equipped with Waters 1515 pump and Waters 2414 differential refractive index detector (set at 30 °C). It used a series of two linear Styragel columns

(HR2 and HR4) at an oven temperature of 45 °C. The eluent was THF at a flow rate of 1.0 mL/min. A series of low-polydispersity polystyrene standards were employed for calibration. Fourier transform infrared (FT-IR) spectra were recorded on a Bruker VECTOR-22 IR spectrometer. The spectra were collected over 64 scans with a spectral resolution of 4 cm^{-1}. Inductively coupled plasma atomic emission spectrometry (ICP-AES) (Perkin-Elmer Corporation Optima 7300 DV) was used for Gd^{3+} content analysis. The particle size distributions were measured using a Zetasizer Nano-ZS (Malvern Instruments, Southborough, MA) with 632.8 nm laser light set at a scattering angle of 173°. All data were averaged over five measurements. All samples were filtered through 0.45 μm Millipore Acrodisc-12 filters to remove dust. The UV absorbance spectra were acquired on a Unico UV/vis 2802PCS spectrophotometer. Fluorescence spectra were recorded using an Hitachi F-4600 spectrofluorometer. The temperature of the water-jacketed cell holder was controlled by a programmable circulation bath. The slit widths were both set at 5 nm for excitation and emission. Transmission electron microscopy (TEM) observations were conducted on a Hitachi H-800 electron microscope at an acceleration voltage of 200 kV. The sample for TEM observations was prepared by placing 10 μL of micellar solution on copper grids coated with thin films of Formvar and carbon successively.

RESULTS AND DISCUSSION

Synthesis of POEGMA-*b*-P(NIPAM-*co*-NBA-*co*-Gd) Diblock Copolymer. Well-defined amphiphilic diblock copolymer, POEGMA-*b*-P(NIPAM-*co*-NBA-*co*-*Gd*), was synthesized by combining consecutive RAFT polymerizations, ring-opening reaction, and "click" functionalization (Scheme 2). POEGMA macroRAFT agent was synthesized at first via the RAFT polymerization of $OEGMA_{475}$ monomer using PDMAT as the chain-transfer agent. The actual DP of the POEGMA macroRAFT agent was estimated to be 18 based on the monomer conversion as determined by ^1H NMR for the crude polymerization mixture before purification. The subsequent RAFT copolymerization of NIPAM, NBA, and GMA was then conducted by utilizing $POEGMA_{18}$ macroRAFT agent. GPC analysis of POEGMA-*b*-P(NIPAM-*co*-NBA-*co*-GMA) diblock copolymer revealed a monomodal and symmetric elution peak (Figure 1b), exhibiting a clear shift to the higher MW region in comparison with that of POEGMA macroRAFT agent (Figure 1a). The FT-IR spectrum of POEGMA-*b*-P(NIPAM-*co*-NBA-*co*-GMA) (Figure S2a of the Supporting Information) showed an absorbance peak at 909 cm^{-1}, which is characteristic of epoxide moieties. The DP of P(NIPAM-*co*-NBA-*co*- GMA) block was determined to be 105 and molar fractions of NIPAM, NBA and GMA moieties were determined to be ∼0.86, ∼0.11, and ∼0.03, respectively, on the basis of ^1H NMR analysis results (Figure S1b of the Supporting Information). After treating POEGMA-*b*-P(NIPAM-*co*-NBA-*co*- GMA) with an excess of AIBN, the subsequent ring-opening reaction with an excess of NaN_3 in the presence of NH_4Cl afforded POEGMA-*b*-P(NIPAM-*co*-NBA-*co*-N_3). In comparison with that of POEGMA-*b*-P(NIPAM-*co*-NBA-*co*-GMA), the presence of azide moieties in POEGMA-*b*-P(NIPAM-*co*-NBA-*co*-N_3) can be evidenced by the appearance of characteristic absorbance peak at ∼2100 cm^{-1}, as shown in the FT-IR spectrum (Figure S2b of the Supporting Information). In addition, the characteristic epoxide absorption peak at ∼909 cm^{-1} completely disappeared after the ring-opening reaction.

The target diblock copolymer, POEGMA-*b*-P(NIPAM-*co*-NBA-*co*-*Gd*), labeled with Gd^{3+} complex in the PNIPAM block was synthesized by "click" functionalization of POEGMA-*b*-P(NIPAM-*co*-NBA-*co*-N_3) with *alkynyl*-DOTA-*Gd*. As shown in Figure 1c, GPC analysis of POEGMA-*b*-P(NIPAM-*co*-NBA-*co*-*Gd*) revealed a monomodal and quite symmetric elution peak, exhibiting a slight shift to the higher MW side in comparison with that of POEGMA-*b*-P(NIPAM-*co*-NBA-*co*-N_3). FT-IR spectrum of POEGMA-*b*- P(NIPAM-*co*-NBA-*co*-*Gd*) (Figure S2c of the Supporting Information) exhibited the absence of azide absorbance peak at ∼2100 cm^{-1}, indicating the complete "click" reaction of azide moieties with *alkynyl*-DOTA-*Gd*. The Gd^{3+} content within the amphiphilic diblock copolymer was determined to be 2.1 wt % by ICP-AES measurement, corresponding to ∼3 DOTA-*Gd* complex per diblock copolymer chain. Therefore, the polymer was denoted as $POEGMA_{18}$-*b*-P($NIPAM_{0.86}$-*co*-$NBA_{0.11}$-*co*-$Gd_{0.03}$)$_{105}$ and shortened as POEGMA-*b*-P(NIPAM-*co*-NBA-*co*-*Gd*).

Micellization of POEGMA-*b*-P(NIPAM-*co*-NBA-*co*-Gd) and UV-Triggered Micellar Disintegration in Aqueous Media. It is well-known that PNIPAM homopolymer exhibits a lower critical solution temperature (LCST) at ∼32 °C. Copolymers of NIPAM with hydrophilic or hydrophobic monomer repeating units will accordingly increase or decrease the LCST compared to that of PNIPAM homopolymer. Previously, Ionov et al.[45,53] incorporated hydrophobic and photocleavable NBA repeating units into thermoresponsive PNIPAM and P(NIPAM-*co*-NBA) copolymer exhibited lower LCSTs compared to that of PNIPAM homopolymer. Upon UV irradiation, the LCST considerably increases relative to that of PNIPAM due to photogenerated acrylic acid (AA) in the ionized form and the formation of P(AA-*co*-NIPAM) copolymer. In the current study, the NBA molar fraction in the P(NIPAM-*co*-NBA-*co*-*Gd*) block is ∼0.11, which renders this block completely hydrophobic (i.e., LCST < 0 °C). This is in reasonable agreement with those report by Ionov et al.,[45] in which the LCST of P(NIPAM-*co*-NBA) at ∼6.0 mol % NBA content already decreases to ∼5 °C. Therefore, POEGMA-*b*-P(NIPAM-*co*-NBA-*co*-*Gd*) behaves as a typical amphiphilic diblock copolymer at room temperature and can self-assemble into core−shell type polymeric micelles consisting of POEGMA coronas and P(NIPAM-*co*- NBA-*co*-*Gd*) cores (Scheme 1). The CMC of POEGMA-*b*-P(NIPAM-*co*-NBA-*co*-*Gd*) micelles was determined to be ∼0.08 g/L at 25 °C via the fluorescence probe method (Figure S3 of the Supporting Information).

Upon UV irradiation of micellar solution, NBA moieties are subjected to photo- cleavage reactions and transform into acrylic acid derivatives, which mainly exist in the ionized form at pH higher than the pK_a. This will lead to micelle microstructural reorganization or even micelle disintegration at high pH due to the prominent increase of LCST for the NIPAM-containing block (Scheme 1). To verify the photocleavage of *o*-nitrobenzyl ester linkages under UV irradiation, the aqueous micellar solution (0.2 g/L, 25 °C) was irradiated with UV light and the kinetics of photochemical reaction was monitored by UV−vis absorption measurements. As shown in Figure 2, UV irradiation led to a decrease in absorption at 265 nm and an increase at 313 nm, clearly demonstrating the cleavage of photolabile *o*-nitrobenzyl ester moieties and the generation of *o*-nitrobenzaldehyde as byproduct, respectively. This is in agreement with previous literature reports.[43,54,55] From Figure 2, we can tell that ∼30 min is needed to complete the UV-induced photochemical reaction.

We then monitored the evolution of size dimensions of polymeric micelles along with the UV irradiation process by dynamic light scattering (DLS). Figure 3a shows the variation

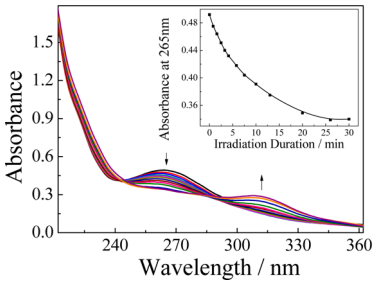

Figure 2. UV absorption spectral changes recorded for the micellar solution (0.2 g/L, 25 °C) of POEGMA-*b*-P(NIPAM-*co*-NBA-*co*-*Gd*) amphiphilic diblock copolymer upon UV irradiation for varying time intervals. Inset: The plot of absorbance at 265 nm against irradiation duration.

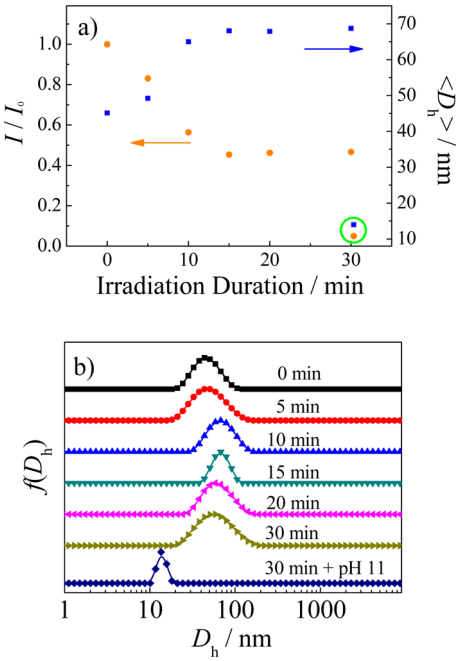

Figure 3. (a) Variation of normalized light scattering intensities (orange circles) and intensity-average hydrodynamic diameters, $<D_h>$ (blue squares), and (b) hydrodynamic diameter distributions recorded for micellar solution (0.2 g/L, 25 °C) of POEGMA-*b*-P(NIPAM-*co*-NBA-*co*-*Gd*) amphiphilic diblock copolymer upon UV irradiation. Data points within the green circle in panel a represent the normalized light scattering intensity and $<D_h>$ recorded for the micellar solution upon 30 min of UV irradiation and adjusting to pH 11, and the corresponding hydrodynamic diameter distribution is shown in panel b.

of normalized light scattering intensities and intensity-average hydrodynamic diameters, $<D_h>$, recorded for micellar solution (0.2 g/L, 25 °C) of POEGMA-*b*- P(NIPAM-*co*-NBA-*co*-*Gd*) upon UV irradiation. Upon UV irradiation, $<D_h>$ increased from ∼45 to ∼68 nm, and the relative light scattering intensities exhibited ∼53% decrease. It is worth noting that after 30 min of UV irradiation, the solution pH decreased to ∼4.6, which should be ascribed to the generation of carboxyl derivatives. On the basis of the above results, we can judge that complete micelle disintegration did not occur upon UV irradiation. This should be ascribed to hydrogen bonding interactions between NIPAM and photogenerated acrylic acid (AA) moieties in the protonated form occurred within micellar cores.[56] Note that the thermal phase transition behavior of P(NIPAM-*co*-AA) random copolymers have been previously reported, and the LCST of which is highly dependent on solution pH.[56,57] However, initially hydrophobic cores of POEGMA-*b*- P(NIPAM-*co*-NBA-*co*-*Gd*) micelles are rendered to be more polar due to newly generated AA residues, thus, micellar nanoparticles are subjected to core swelling (Scheme 1 and Figure 3).

To verify the above assumption, we conducted potentiometric titration for the aqueous solution of POEGMA-*b*-P(NIPAM-*co*-NBA-*co*-*Gd*) after subjected to 30 min of UV irradiation, which can transform all NBA residues into AA moieties (Figure 2). As shown in Figure S4 of the Supporting Information, the pK_a of UV-irradiated diblock copolymer was determined to be ∼4.4, which agrees with relevant literature reports.[58−60] This confirmed the presence of protonated carboxylate residues after UV irradiation of the micellar solution, the pH of which was initially at 7.4 but decreased to ∼pH 4.6 after irradiation. This indicates that ∼50% of photogenerated carboxylate residues remained to be protonated. The presence of hydrogen bonding interactions within micellar cores after UV irradiation prevented complete micellar disintegration. This can be further evidenced from the fact that after adjusting the photoirradiated aqueous solution to pH 11 DLS measurements revealed quite low scattering intensity (5% relative to that prior to irradiation) and an $<D_h>$ of ∼13.5 nm corresponding to molecularly dissolved unimers (Figure 3). At pH 11, all carboxylate residues remain ionized, and there exists no hydrogen bonding or other favorable interactions within micellar cores. Therefore, complete micellar disintegration occurs.

To explore the microenvironmental polarity changes for POEGMA-*b*-P(NIPAM-*co*-NBA-*co*-*Gd*) micelles upon UV irradiation, we utilized Nile red as a polarity-sensitive fluorescence probe. Evolution of fluorescence emission spectra (λ_{ex} = 550 nm) of Nile red-loaded micelles (0.2 g/L, 25 °C) in PBS buffer (pH 7.4) upon UV irradiation was shown in Figure 4a. The solubility of Nile red in pure water is limited, and the emission peak maximum is 657 nm in the absence of polymeric micelles. In the micellar solution, the fluorescence intensity of Nile red increases ∼22-fold, and the emission peak maximum blue-shifts to ∼627 nm. Upon UV irradiation, the emission intensity prominently decreases with increasing irradiation duration, accompanied by a red shift in emission spectra. This indicates the release of Nile red from hydrophobic micellar cores to the bulk aqueous phase and that micellar cores are getting more polar.[43,55] In contrast, there exist almost no changes in emission intensity for the micellar solution stored in dark (Figure 4b). The observed photoregulated release of Nile red suggested POEGMA-*b*-P(NIPAM-*co*-NBA-*co*-*Gd*) micelles can be used for the delivery and controlled release of hydrophobic chemotherapeutic drugs. We can also tell from Figure 4a that complete Nile red release cannot be achieved even after ∼30 min of UV irradiation. This is in reasonable agreement with the DLS data recorded for UV-irradiated micellar solution, as shown in Figure 3, which revealed the presence of aggregates stabilized by hydrogen-bonding interactions within nanoparticle cores.

In Vitro MR Imaging Relaxivity Measurement. The longitudinal relaxation rates ($1/T_1$) of POEGMA-*b*-P(NIPAM-*co*-NBA-*co*-*Gd*) micelles at varying Gd^{3+} concentrations (0, 0.01, 0.02, 0.03, and 0.04 mM) after UV irradiation for different time durations (0, 15, and 30 min) was then measured. It is clearly evident from T_1-weighted MR images (Figure 5a) that

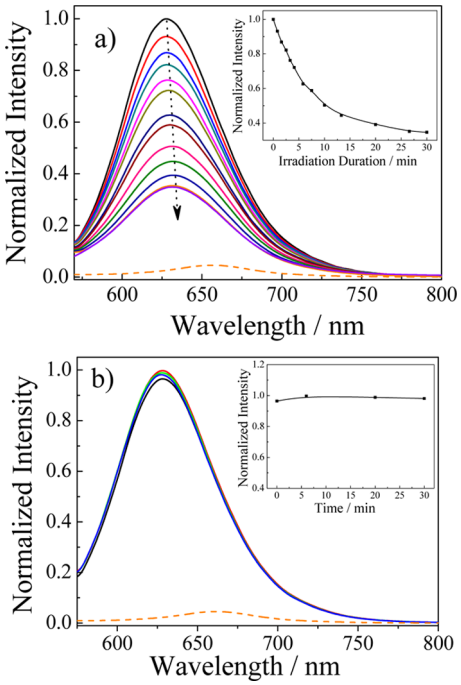

Figure 4. Evolution of fluorescence emission spectra (λ_{ex} = 550 nm) of Nile Red-loaded POEGMA-*b*-P(NIPAM-*co*-NBA-*co*-*Gd*) diblock copolymer micelles (0.2 g/L, 25 °C): (a) upon UV irradiation and (b) kept in dark for varying time intervals. Insets: time-dependent changes in normalized emission intensities of Nile red at 628 nm (excitation wavelength 550 nm). The baseline represents the emission spectrum of Nile Red in pure water. Nile Red concentration is fixed to be 6.6 × 10^{-7} M in all cases.

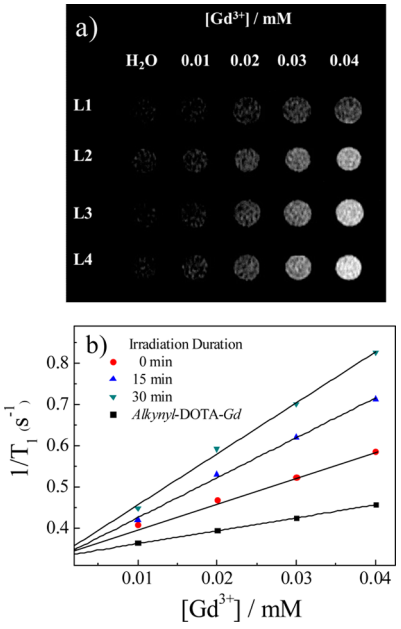

Figure 5. Gd^{3+} concentration dependent (a) T_1-weighted MR images (magnetic strength: 1.5 T; TR = 300 ms, TE = 10 ms) and (b) water proton longitudinal relaxation rate ($1/T_1$) recorded for (L1) *Alkynyl*-DOTA-*Gd*, and POEGMA-*b*-P(NIPAM-*co*-NBA-*co*-*Gd*) diblock copolymer micellar solutions (25 °C) (L2) before and after UV irradiation for (L3) 15 min and (L4) 30 min.

the longer the irradiation time, the more prominent positive contrast can be achieved for POEGMA-*b*-P(NIPAM-*co*-NBA-*co*-*Gd*) micelles at the same [Gd^{3+}] concentration. T_1 relaxivity, r_1, was then determined from the slope of $1/T_1$ versus [Gd^{3+}] plot (Figure 5b). r_1 values of *alkynyl*-DOTA-*Gd* and POEGMA-*b*-P(NIPAM-*co*-NBA-*co*-*Gd*) micelles before and after irradiation for 15 and 30 min were then calculated to be 3.1, 6.5, 9.7, and 12.1 mM^{-1} s^{-1}, respectively.

For POEGMA-*b*-P(NIPAM-*co*-NBA-*co*-*Gd*) micelles, DOTA-*Gd* complexes are covalently embedded within hydrophobic cores, and thus, water exchange between DOTA-*Gd* complex and water molecules will be considerably affected. We have hypothesized that the MR contrast performance of micelles prior to UV irradiation will be less prominent compared with that of small molecule Gd complexes. However, the r_1 of POEGMA-*b*- P(NIPAM-*co*-NBA-*co*-*Gd*) micelles (6.5 $mM^{-1}s^{-1}$) is higher than that of *alkynyl*-DOTA-*Gd* (r_1 = 3.1 mM^{-1} s^{-1}).[42] This might be ascribed to the fact that P(NIPAM-*co*-NBA-*co*-*Gd*) micellar cores are not hydrophobic enough and DOTA-*Gd* complexes are still partially accessible to water molecules. In addition, the micellar cores contain many *alkynyl*- DOTA-*Gd* complexes due to the multimolecular chain aggregation nature, and this can contribute to enhanced T_1 relaxivity relative to that of small molecule *alkynyl*-DOTA-*Gd*. Note that this effect has been well-documented in literature reports.[1,2,4]

Upon UV irradiation, micellar cores are subjected to swelling and hydrophobic-to-hydrophilic transitions (Scheme 1). At 15 and 30 min of irradiation duration, r_1 values increased to 9.7 and 12.1 mM^{-1} s^{-1}, respectively. The considerable MR contrast enhancement along with the photoirradiation process can be interpreted as follows: (1) the transformation of hydrophobic *o*-nitrobenzyl acrylate moieties into hydrophilic carboxylate derivatives rendered water molecules more accessible to the open coordination site of DOTA-*Gd* complex; (2) the presence of aggregate nanostructures stabilized by hydrogen bonding interactions after UV irradiation (Figure 3) can further restrict the rotational mobility of DOTA-*Gd* complexes, which is also advantageous for the enhancement of T_1 relaxivity.

Photo-Regulated Doxorubicin Release Profile and Cytotoxicity of Drug-Loaded Micelles. In the next step, we investigated drug release profiles and cytotoxicity of Dox-loaded micelles. Figure 6a shows the D_h distribution of Dox-loaded diblock copolymer micelles in aqueous solution (0.2 g/L, 25 °C), exhibiting an <D_h> of 51 nm and a size polydispersity (μ_2/Γ^2) of <0.1. Drug-loaded micelles are slightly larger than that of empty micelles (45 nm). The TEM image shown in Figure 6a revealed the presence of spherical nanoparticles of narrow size distribution for drug-loaded micelles, and the average diameter was estimated to be ~26 nm, which generally agrees with the DLS data considering that the former reflects micelle size dimension in the dry state.

To calculate the drug LC% and the EE%, we recorded the fluorescence emission spectrum of dialysates to determine the amount of unloaded Dox against a standard calibration curve.[40] For micelles self-assembled from POEGMA-*b*-P(NIPAM-*co*-NBA-*co*-*Gd*), the EE% and LC% values were determined to be 86.0 and 4.9%, respectively. Figure 6b shows the cumulative Dox release profiles from drug-loaded micelles under varying conditions. At 37 °C and pH 7.4 buffer, ~47% of loaded drug can be released over 25 h for micelles prior to UV irradiation, whereas for Dox-loaded micelles after UV irradiation for 30 min enhanced release rate of Dox can be clearly observed and ~68% release of loaded drug in 25 h was achieved. In addition, ~65% Dox release actually occurred within the first 12 h. In

dx.doi.org/10.1021/bm301425j | *Biomacromolecules* 2012, 13, 3877−3886

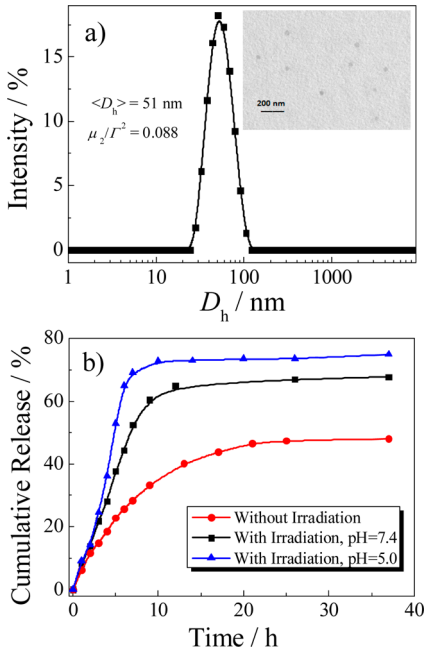

Figure 6. (a) Hydrodynamic diameter, D_h, distribution of Dox-loaded POEGMA-*b*-P(NIPAM-*co*-NBA-*co*-Gd) diblock copolymer micelles in aqueous solution (0.2 g/L, 25 °C). Inset: typical TEM image of Dox-loaded micelles. (b) Cumulative Dox release profile from drug-loaded micelles (1.0 g/L, pH 7.4 or 5.0 buffer; 37 °C; drug loading content: 4.9 wt/wt %) without and with UV irradiation for 30 min.

combination with results obtained for light-regulated Nile red release from micelles (Figure 4), the enhanced Dox release rate should be ascribed to light-triggered hydrophobic−hydrophilic transition within micellar cores and the concomitant core swelling event (Figure 3).

Considering that upon cellular uptake of drug-loaded POEGMA-*b*-P(NIPAM-*co*- NBA-*co*-Gd) micelles, they are subjected to transport through acidic intracellular organelles such as endosomes and lysosomes (pH ∼5 to 6). We then measured the drug release profile of POEGMA-*b*-P(NIPAM-*co*-NBA-*co*-Gd) micelles in pH 5.0 buffer media with 30 min of UV irradiation (Figure 6b). It was found that at pH 5.0 the drug release rate was enhanced (∼73% cumulative release over 12 h) compared with that at pH 7.4 (∼65% release over 12 h). For UV-irradiated micellar dispersion, the pK_a of newly generated AA moieties was determined to be ∼4.4 (Figure S4 of the Supporting Information). Therefore, the micellar nanoparticles possess more negative charges at pH 7.4 compared with that at pH 5.0 after UV irradiation. Considering that Dox has a pK_a of ∼8.2 (i.e., they are positively charged to some extent), the decrease in electrostatic interactions between AA moieties and Dox at pH 5.0 can result in more prominent Dox release from UV-irradiated micellar dispersion.[52] This also implies the increase in chemotherapeutic efficacy by exploiting the transport pathway of micellar nanocarriers through acidic organelles such as endosomes and lysosomes.

Finally, we examined the in vitro cell cytotoxicity of POEGMA-*b*-P(NIPAM-*co*-NBA-*co*-Gd) micelles via the MTT assay against HepG2 cells (Figure 7). The cell viability of drug-free blank micelles with and without UV irradiation remained to be ∼88% at a polymer concentration of 3.0 g/L, revealing that block copolymer micellar nanocarriers are almost non-cytotoxic. When HepG2 cells were incubated with Dox-loaded micelles without UV irradiation, ∼48% cells survived at a final

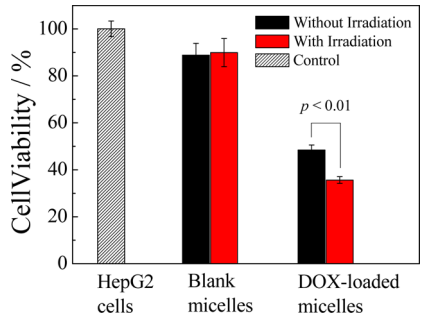

Figure 7. Comparison of MTT cytotoxicity assay results of HepG2 cells against blank and Dox-loaded micellar solution of POEGMA-*b*-P(NIPAM-*co*-NBA-*co*-Gd) diblock copolymer at a concentration of 3.0 mg/mL: (dark bar) without irradiation and (red bar) with 365 nm UV irradiation for 30 min.

polymer concentration of 3.0 g/L, indicating that Dox-loaded micelles are therapeutically active to HepG2 cells. When the incubation mixture was subjected to 30 min of light irradiation, the cell viability decreased further and only ∼36% cells survived. The statistically significance difference could be confirmed by Student's t test with $p < 0.01$, indicating that Dox-loaded micelles exhibited enhanced drug release upon UV irradiation. This is also in agreement with the discrepancy in drug release profiles for nonirradiated and irradiated micellar dispersions (Figure 6).

This conclusion was further corroborated via the DAPI nuclear stain technique. Figure 8 shows CLSM images recorded for HepG2 cells after incubation for 12 h in the absence (Figure 8a) and presence of Dox-loaded micelles without (Figure 8b) and with (Figure 8c) 30 min of UV irradiation. For cells treated

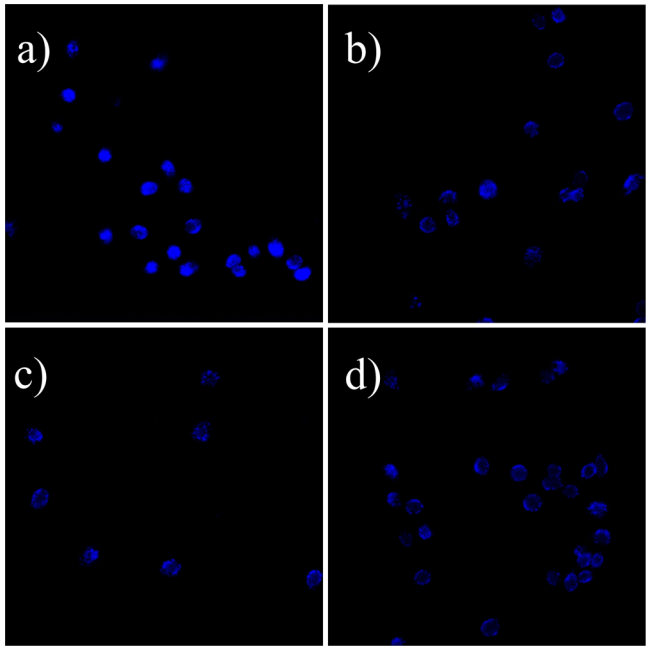

Figure 8. Dox-loaded micelles induced apoptosis of HepG2 cells as detected by DAPI nuclear staining (405 nm excitation; 440−480 nm blue channel). CLSM images of HepG2 cells after incubation for 12 h in the absence (a) and presence of drug-loaded micelles without (b) and with (c) 365 nm UV irradiation for 30 min. In panel d, the cells were pretreated with 100 μM Ac-DEVD-CHO for 2 h and then treated with drug-loaded micelles with 30 min UV irradiation.

dx.doi.org/10.1021/bm301425j | *Biomacromolecules* 2012, 13, 3877−3886

with Dox-loaded micelles and subjected to 30 min irradiation, the cell survival rate is the lowest, which agrees with the MTT assay results (Figure 7). As a control (Figure 8d), the cells were pretreated with 100 μM Ac-DEVD-CHO, which can act as a caspase inhibitor in the process of caspase-induced apoptosis and then treated with Dox-loaded micelles and subjected to 30 min UV irradiation. The cells were then stained by DAPI following standard protocols and imaged by CLSM. As expected, the presence of Ac-DEVD-CHO can effectively protect HepG2 cells from Dox-related apoptosis.

CONCLUSIONS

In summary, we synthesized POEGMA-*b*-P(NIPAM-*co*-NBA-*co*-Gd) amphiphilic diblock copolymer via the combination of consecutive RAFT polymerizations and "click" postfunctionalization at first. Self-assembled micelles of as-prepared diblock copolymer were further used to encapsulate physically a hydrophobic drug (Dox). Before UV irradiation, micellar nanoparticles exhibit only moderate drug release rate (~47% Dox release in 25 h) and a longitudinal relaxivity (r_1) of ~6.5 mM^{-1} s^{-1}. UV irradiation of the micellar dispersion triggers hydrophobic−hydrophilic transition for micellar cores associated with core swelling. Accordingly, accelerated drug release rate (~65% of Dox release in 12 h upon 30 min UV irradiation) and enhanced T_1 contrast performance ($r_1 \approx 9.7$ and 12.1 mM^{-1} s^{-1} for 15 and 30 min UV irradiation, respectively) were observed. The irradiation duration-dependent T_1 contrast performance clearly reflects the microstructural changes of micellar cores upon UV irradiation. We expect that the further integration of the current design with near-infrared-cleavable moieties will render the reported theranostic nanocarriers with improved tissue penetration and more appropriate for real clinical applications.

ASSOCIATED CONTENT

Supporting Information

^{1}H NMR, FT-IR, potentiometric titration, and probe fluorescence results. This material is available free of charge via the Internet at http://pubs.acs.org.

AUTHOR INFORMATION

Corresponding Author

*E-mail: sliu@ustc.edu.cn.

Notes

The authors declare no competing financial interest.

ACKNOWLEDGMENTS

This work is supported by National Natural Scientific Foundation of China (NNSFC) Project (51033005, 91027026, and 21274137) and Fundamental Research Funds for the Central Universities

REFERENCES

(1) Khemtong, C.; Kessinger, C. W.; Gao, J. M. *Chem. Commun.* **2009**, 3497−3510.
(2) Datta, A.; Raymond, K. N. *Acc. Chem. Res.* **2009**, *42*, 938−947.
(3) Caravan, P.; Ellison, J. J.; McMurry, T. J.; Lauffer, R. B. *Chem. Rev.* **1999**, *99*, 2293−2352.
(4) Villaraza, A. J. L.; Bumb, A.; Brechbiel, M. W. *Chem. Rev.* **2010**, *110*, 2921−2959.
(5) Luo, K.; Liu, G.; She, W. C.; Wang, Q. Y.; Wang, G.; He, B.; Ai, H.; Gong, Q. Y.; Song, B.; Gu, Z. W. *Biomaterials* **2011**, *32*, 7951−7960.
(6) Yang, X. Q.; Grailer, J. J.; Rowland, I. J.; Javadi, A.; Hurley, S. A.; Matson, V. Z.; Steeber, D. A.; Gong, S. Q. *ACS Nano* **2010**, *4*, 6805−6817.
(7) Ai, H.; Flask, C.; Weinberg, B.; Shuai, X.; Pagel, M. D.; Farrell, D.; Duerk, J.; Gao, J. M. *Adv. Mater.* **2005**, *17*, 1949.
(8) Caravan, P. *Acc. Chem. Res.* **2009**, *42*, 851−862.
(9) De Leon-Rodriguez, L. M.; Lubag, A. J. M.; Malloy, C. R.; Martinez, G. V.; Gillies, R. J.; Sherry, A. D. *Acc. Chem. Res.* **2009**, *42*, 948−957.
(10) Kim, T.; Cho, E. J.; Chae, Y.; Kim, M.; Oh, A.; Jin, J.; Lee, E. S.; Baik, H.; Haam, S.; Suh, J. S.; Huh, Y. M.; Lee, K. *Angew. Chem., Int. Ed.* **2011**, *50*, 10589−10593.
(11) Zhang, S. R.; Wu, K. C.; Sherry, A. D. *Angew. Chem., Int. Ed.* **1999**, *38*, 3192−3194.
(12) Rodriguez, E.; Nilges, M.; Weissleder, R.; Chen, J. W. *J. Am. Chem. Soc.* **2010**, *132*, 168−177.
(13) Moats, R. A.; Fraser, S. E.; Meade, T. J. *Angew. Chem., Int. Ed. Engl.* **1997**, *36*, 726−728.
(14) Zhang, X. A.; Lovejoy, K. S.; Jasanoff, A.; Lippard, S. J. *Proc. Natl. Acad. Sci. U. S. A.* **2007**, *104*, 10780−10785.
(15) Atanasijevic, T.; Shusteff, M.; Fam, P.; Jasanoff, A. *Proc. Natl. Acad. Sci. U. S. A.* **2006**, *103*, 14707−14712.
(16) Zhao, Y. *Macromolecules* **2012**, *45*, 3647−3657.
(17) Rapoport, N. *Prog. Polym. Sci.* **2007**, *32*, 962−990.
(18) Pasparakis, G.; Manouras, T.; Argitis, P.; Vamvakaki, M. *Macromol. Rapid Commun.* **2012**, *33*, 183−198.
(19) Zhao, H.; Sterner, E. S.; Coughlin, E. B.; Theato, P. *Macromolecules* **2012**, *45*, 1723−1736.
(20) Johnson, J. A.; Lu, Y. Y.; Burts, A. O.; Lim, Y. H.; Finn, M. G.; Koberstein, J. T.; Turro, N. J.; Tirrell, D. A.; Grubbs, R. H. *J. Am. Chem. Soc.* **2011**, *133*, 559−566.
(21) Koylu, D.; Thapa, M.; Gumbley, P.; Thomas, S. W. *Adv. Mater.* **2012**, *24*, 1451−1454.
(22) Liu, G.; Dong, C. M. *Biomacromolecules* **2012**, *13*, 1573−1583.
(23) Cabane, E.; Malinova, V.; Menon, S.; Palivan, C. G.; Meier, W. *Soft Matter* **2011**, *7*, 9167−9176.
(24) Tu, C. Q.; Louie, A. Y. *Chem. Commun.* **2007**, 1331−1333.
(25) Osborne, E. A.; Jarrett, B. R.; Tu, C. Q.; Louie, A. Y. *J. Am. Chem. Soc.* **2010**, *132*, 5934.
(26) Prabaharan, M.; Grailer, J. J.; Pilla, S.; Steeber, D. A.; Gong, S. Q. *Biomaterials* **2009**, *30*, 3009−3019.
(27) Meng, F. H.; Hennink, W. E.; Zhong, Z. *Biomaterials* **2009**, *30*, 2180−2198.
(28) Cheng, D.; Cao, N.; Chen, J. F.; Yu, X. S.; Shuai, X. T. *Biomaterials* **2012**, *33*, 1170−1179.
(29) Peer, D.; Karp, J. M.; Hong, S.; FarokHzad, O. C.; Margalit, R.; Langer, R. *Nat. Nanotechnol.* **2007**, *2*, 751−760.
(30) Sumer, B.; Gao, J. M. *Nanomedicine* **2008**, *3*, 137−140.
(31) Guthi, J. S.; Yang, S. G.; Huang, G.; Li, S. Z.; Khemtong, C.; Kessinger, C. W.; Peyton, M.; Minna, J. D.; Brown, K. C.; Gao, J. M. *Mol. Pharmaceutics* **2010**, *7*, 32−40.
(32) Blanco, E.; Kessinger, C. W.; Sumer, B. D.; Gao, J. *Exp. Biol. Med.* **2009**, *234*, 123−131.
(33) Lammers, T.; Aime, S.; Hennink, W. E.; Storm, G.; Kiessling, F. *Acc. Chem. Res.* **2011**, *44*, 1029−1038.
(34) Sanson, C.; Diou, O.; Thevenot, J.; Ibarboure, E.; Soum, A.; Brulet, A.; Miraux, S.; Thiaudiere, E.; Tan, S.; Brisson, A.; Dupuis, V.; Sandre, O.; Lecommandoux, S. *ACS Nano* **2011**, *5*, 1122−1140.
(35) Weinberg, B. D.; Patel, R. B.; Exner, A. A.; Saidel, G. A.; Gao, J. M. *J. Controlled Release* **2007**, *124*, 11−19.
(36) Gao, G. H.; Im, G. H.; Kim, M. S.; Lee, J. W.; Yang, J.; Jeon, H.; Lee, J. H.; Lee, D. S. *Small* **2010**, *6*, 1201−1204.
(37) Nakamura, E.; Makino, K.; Okano, T.; Yamamoto, T.; Yokoyama, M. *J. Controlled Release* **2006**, *114*, 325−333.
(38) Takaoka, Y.; Kiminami, K.; Mizusawa, K.; Matsuo, K.; Narazaki, M.; Matsuda, T.; Hamachi, I. *J. Am. Chem. Soc.* **2011**, *133*, 11725−11731.
(39) Li, C. H.; Zhang, Y. X.; Hu, J. M.; Cheng, J. J.; Liu, S. Y. *Angew. Chem., Int. Ed.* **2010**, *49*, 5120−5124.

(40) Wan, X. J.; Liu, T.; Liu, S. Y. *Biomacromolecules* **2011**, *12*, 1146−1154.
(41) Hu, J. M.; Dai, L.; Liu, S. Y. *Macromolecules* **2011**, *44*, 4699−4710.
(42) Li, X. J.; Qian, Y. F.; Liu, T.; Hu, X. L.; Zhang, G. Y.; You, Y. Z.; Liu, S. Y. *Biomaterials* **2011**, *32*, 6595−6605.
(43) Jiang, J. Q.; Tong, X.; Morris, D.; Zhao, Y. *Macromolecules* **2006**, *39*, 4633−4640.
(44) Ramanan, V. V.; Katz, J. S.; Guvendiren, M.; Cohen, E. R.; Marklein, R. A.; Burdick, J. A. *J. Mater. Chem.* **2010**, *20*, 8920−8926.
(45) Ionov, L.; Diez, S. *J. Am. Chem. Soc.* **2009**, *131*, 13315−13319.
(46) Li, C. H.; Ge, Z. S.; Fang, J.; Liu, S. Y. *Macromolecules* **2009**, *42*, 2916−2924.
(47) Du, J. Z.; Tang, L. Y.; Song, W. J.; Shi, Y.; Wang, J. *Biomacromolecules* **2009**, *10*, 2169−2174.
(48) Jiang, X.; Lavender, C. A.; Woodcock, J. W.; Zhao, B. *Macromolecules* **2008**, *41*, 2632−2643.
(49) Mohan, P.; Rapoport, N. *Mol. Pharmaceutics* **2010**, *7*, 1959−1973.
(50) Sun, H. L.; Guo, B. N.; Cheng, R.; Meng, F. H.; Liu, H. Y.; Zhong, Z. Y. *Biomaterials* **2009**, *30*, 6358−6366.
(51) Sun, H. L.; Guo, B. N.; Li, X. Q.; Cheng, R.; Meng, F. H.; Liu, H. Y.; Zhong, Z. Y. *Biomacromolecules* **2010**, *11*, 848−854.
(52) Knezevic, N. Z.; Trewyn, B. G.; Lin, V. S. Y. *Chem.—Eur. J.* **2011**, *17*, 3338−3342.
(53) Ionov, L.; Synytska, A.; Diez, S. *Adv. Funct. Mater.* **2008**, *18*, 1501−1508.
(54) Han, G.; You, C. C.; Kim, B. J.; Turingan, R. S.; Forbes, N. S.; Martin, C. T.; Rotello, V. M. *Angew. Chem., Int. Ed.* **2006**, *45*, 3165−3169.
(55) Yesilyurt, V.; Ramireddy, R.; Thayumanavan, S. *Angew. Chem., Int. Ed.* **2011**, *50*, 3038−3042.
(56) Burova, T. V.; Grinberg, N. V.; Grinberg, V. Y.; Kalinina, E. V.; Lozinsky, V. I.; Aseyev, V. O.; Holappa, S.; Tenhu, H.; Khokhlov, A. R. *Macromolecules* **2005**, *38*, 1292−1299.
(57) Weng, Y. M.; Ding, Y. W.; Zhang, G. Z. *J. Phys. Chem. B* **2006**, *110*, 11813−11817.
(58) Kurkuri, M. D.; Aminabhavi, T. M. *J. Controlled Release* **2004**, *96*, 9−20.
(59) Hu, Y.; Ding, Y.; Ding, D.; Sun, M. J.; Zhang, L. Y.; Jiang, X. Q.; Yang, C. Z. *Biomacromolecules* **2007**, *8*, 1069−1076.
(60) Ishiduki, K.; Esumi, K. *Langmuir* **1997**, *13*, 1587−1591.